Breakout and Breakdown Induced by Crystallization in Cylinder-Forming Diblock Copolymers

Yong Qian, Tao Cai, and Wenbing Hu*

Department of Polymer Science and Engineering, State Key Laboratory of Coordination Chemistry, School of Chemistry and Chemical Engineering, Nanjing University, Nanjing 210093, China

Received May 16, 2008; Revised Manuscript Received July 12, 2008

ABSTRACT: We report dynamic Monte Carlo simulations of polymer crystallization confined softly in cylindrical microdomains of diblock copolymers. We observed both the breakout that generally raises coalescence of microdomains and the breakdown that uniquely turns cylinders into strings of single crystallites. They can be monitored by the disappearance of structure factors at the wave vector of the square root of seven with reference to the highest peak of structure factors. By comparison of two cases with and without the postgrowth crystal thickening, we found that for those tilted or perpendicular-oriented crystals in cylinders their postgrowth isothermal thickening makes the breakout, while their lateral crystal growth is responsible for the breakdown if the growth thickness goes beyond the thickness of cylinders. The results may facilitate our better understanding of the morphological control in the crystallization of cylinder-forming diblock copolymers.

I. Introduction

It is well-known that the self-assembly of asymmetric diblock copolymers yields nanoscale arrays of cylinders under proper segregation strengths and compositions in the bulk phase. These arrays of nanowires have many potential applications in such as the microelectronics, the device technology, and the drug delivery.[1−3] However, the industrial realization of their applications is very much related with the availability of a large-scale uniform nanopattern upon fabrication. Crystallization of polymers happens under such a quasi-one-dimensional spatial confinement.[4,5] Under a soft confinement, crystallization of polymers often gives rise to the so-called breakout in the cylindrical microdomains of diblock copolymers[6−11] and thus be one of the essential factors responsible for the ruin of nanopatterns.

Recently, the observation under atomic force microscopy (AFM) found another kind of frustration that is unique to the fabrication of nanoarrays of cylinders: the cylinders are broken down into strings of small microdomains induced by the crystallization or annealing at high temperatures.[12] Such a behavior changes the nanopattern in the range limited inside each cylinder, unlike the breakout which makes coalescence of cylinders. Up to now, the microscopic mechanisms for both the breakout and breakdown in the cylindrical microdomains of diblock copolymers have not yet been clearly studied.

Molecular simulations are powerful tools to gain insights into this sort of microscopic mechanism of polymers. We hereby employ dynamic Monte Carlo simulations of lattice polymers to address the above issue. The method has been applied to study the breakout of lamellar microdomains of diblock copolymers[13] where the postgrowth isothermal thickening of the perpendicular-oriented crystals appears to be responsible for the coalescence of lamellar microdomains at high temperatures. The same approaches have also been applied to study the crystal orientations under hard confinement of cylindrical microdomains of diblock copolymers.[14] In the sense of experiments, the soft confinement is realized by the diblock copolymers with the glass transition temperature of the noncrystallizable block lower than the crystallization temperature of another block.[15] We directly make use of the cylindrical microdomains of diblock copolymers prepared in the previous simulations to study polymer crystallization under soft confinement. To monitor the breakout and breakdown in our simulations, the disappearance of structure factors at the wave vector of the square root of seven referenced to the wave vector of the highest peak of structure factors will be watched. The comparison between two cases with and without crystal thickening reveals that the breakout can be assigned to the isothermal thickening of those tilted or perpendicular-oriented crystals after crystal growth, while the breakdown is attributed to the lateral crystal growth of those tilted or perpendicular-oriented crystals with their growing thickness larger than the thickness of cylinders.

In this paper, after the introduction, we make a brief description to the simulation techniques, followed with the report of simulation results and some discussions. The paper ends up with a summary of our conclusions.

II. Simulation Techniques

Dynamic Monte Carlo simulations have been widely applied in the study of crystallization behaviors of polymers.[16] In this approach, polymer chains are moving via the microrelaxation model in the lattice space with periodic boundary conditions. The microrelaxation model allows the monomer jumping into its vacancy neighbor, sometimes with partial sliding diffusion along the local chain. Double occupations of monomers and the overcrossing of bonds are forbidden to mimic the volume exclusions of polymer chains. 7860 chains, each containing 32 monomers, were put into a 64^3 cubic lattice and then were allowed to relax into the bulk amorphous phase under athermal conditions.

We first prepared the cylindrical microdomains by initiating the spontaneous microphase separation in the bulk amorphous phase and then studied the crystallization under soft confinement of cylinders. To this end, we employed the conventional Metropolis sampling algorithm with the potential energy barrier composed as

* Corresponding author: E-mail address: wbhu@nju.edu.cn.

10.1021/ma801097y CCC: $40.75
Published on Web 09/04/2008

$$\frac{\Delta E}{kT} = \frac{bB + pE_p + cE_c + \sum_i f(i)E_r}{kT} = \left(b\frac{B}{E_c} + p\frac{E_p}{E_c} + c + \sum_i f(i)\frac{E_r}{E_c}\right)\frac{E_c}{kT} \quad (1)$$

where B is the mixing interaction between the monomers of two different components, E_p is the nonparallel packing energy for the pair of bonds in the crystallizable component, E_c is the noncollinear connection energy for the pair of bonds consecutively connected along the chain, E_r is the frictional barrier for the bond in the path of local sliding diffusion, b, p, and c are the net changes of the number in each step of microrelaxation, $f(i)$ is the number of parallel crystallizable bonds around each crystallizable bond in sliding diffusion, the summation is integrated over all the contributions of those parallel bonds along the path of local sliding diffusion, k is the Boltzmann constant, and T is the temperature. In practice, we set B/E_c to adjust the segregation strength and gave $E_p/E_c = 1$ and $E_r/E_c = 0.3$ only to those crystallizable bonds. $E_r/E_c = 0.3$ was chosen to block any crystal thickening via sliding diffusion of polymer chains after crystal growth,[17] in comparison to the case of $E_r/E_c = 0$ where the crystal thickening may dominate the coalescence of cylinders. $E_c/(kT)$ was programmed as the reduced temperature.

In previous simulations,[14] we have searched through the phase diagrams of the various-shaped microdomains of the above diblock copolymer systems with variable compositions and found the well-defined hexagonal array of cylindrical microdomains for an asymmetric diblock copolymer with the first nine monomers crystallizable and the remaining 23 monomers noncrystallizable, after performing microphase separation at $B/E_c = 0.5$ and $kT/E_c = 4.8$ (other energy parameters were temporarily set as zero), for 8×10^5 Monte Carlo (MC) cycles (each MC cycle was defined as the number of trial moves equal to the total number of sites in the lattice box). We directly made use of the prepared cylindrical microdomains as the spatial template for crystallization under soft confinement by switching on $E_p/E_c = 1$ to the crystallizable blocks. The hard confinement is realized by rejecting all the microrelaxation involving the noncrystallizable blocks. In the present simulations, we study the case of $E_r/E_c = 0$ for crystallization with significant crystal thickening, in comparison to the case of $E_r/E_c = 0.3$ for crystallization without postgrowth crystal thickening.

Since in our simulations the parallel packing of the crystallizable bonds represented the crystalline order, we monitored the crystallization by tracing the crystallinity that was defined as the fraction of crystallizable bonds containing more than five parallel crystallizable neighbors. We also calculated the orientational-order parameters defined as

$$P = \frac{3\langle \cos^2 \theta \rangle - 1}{2} \quad (2)$$

where the angle is referenced to long axis of the cylinders and $\langle ... \rangle$ makes an ensemble average over those crystalline bonds containing more than five parallel crystallizable neighbors. If all the crystalline bonds are parallel to the cylinders, $P = 1$; if those bonds are perpendicular to the cylinders, $P = -0.5$; and if all the bonds are randomly oriented, $P = 0$.

We further traced the time evolution of the collective structure factors defined as the spherically averaged one-dimensional results, as given by

$$S(q,t) = \frac{1}{3L^3}\sum_{j,k} \exp(iq \cdot r_{jk}) \langle \sigma(r_j,t)\, \sigma(r_k,t) \rangle \quad (3)$$

where q is the wave vector with discrete integers times $2\pi/L$, t is the time, L is the linear size of the cubic box, and the sum is taken over all pairs of the lattice sites with a distance r. If a lattice pair was occupied by the crystallizable monomers, $\sigma = 1$, and if containing other species, $\sigma = 0$. The structure factors have been familiar as the scattering intensity in those small-angle X-ray scattering measurements on the corresponding experimental systems. The quantity expressed in eq 3 has been applied to study microphase separation of asymmetric diblock copolymers.[18]

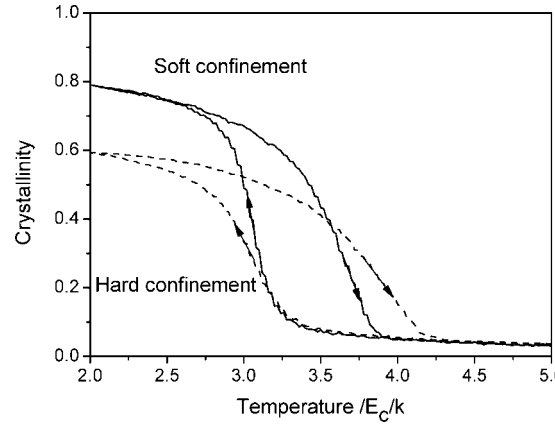

Figure 1. Comparisons of the cooling and heating curves of crystallinity under soft and hard confinements, respectively, for the cylindrical microdomains of diblock copolymers. $B/E_c = 0.4$, $E_p/E_c = 1$, and $E_r/E_c = 0$. The hard confinement was realized by prohibiting all the trials of microrelaxation involving the noncrystallizable component. The arrows on the curves indicate the directions of stepwise scanning of the temperature with step length 0.02 and step period 500 MC cycles. The crystallinity was calculated at the end of each temperature step. Only the segments connecting the data at each step are shown for clarity.

III. Results and Discussion

We first observed the cooling and heating curves of crystallinity under both hard and soft confinement. The results are shown in Figure 1. One can see that the soft confinement makes both higher crystallization and melting rates (larger slopes of curves in the transition regions) than the hard confinement. In addition, under soft confinement, a higher crystallinity can be approached at low temperatures. These results are consistent with the experimental observations on cylinder-forming poly(ethylene oxide)-*block*-polystyrene[19] and similar to the previous simulations of lamellar diblock copolymers.[13] The slowness of phase transitions under hard confinement can be attributed to the frozen block junction that restricts the mobility of the crystallizable block.

Next, we quenched the cylinders into various low temperatures for isothermal crystallization under soft confinement. The crystallinity and orientational-order parameters after the saturated crystallization have been calculated, as summarized in Figure 2. One can see that with the increase of crystallization temperatures the crystallinity decreases and the crystals prefer to become tilted and even more perpendicular-oriented at high temperatures. These results are similar to the previous simulations of cylindrical diblock copolymers under hard confinement.[14] It has been identified that at high temperatures the preferences of crystal orientation perpendicular to the cylinders can be attributed to the crystal nucleation induced by the perpendicular-oriented block junctions at the interfaces.[14]

We then went to the details of isothermal crystallization at the high temperature 3.35 for the case without any sliding restriction in the crystalline phase, i.e. $E_r/E_c = 0$. The time evolution of crystallinity at this temperature is shown in Figure 3. One can thus define the saturated point of crystallization by

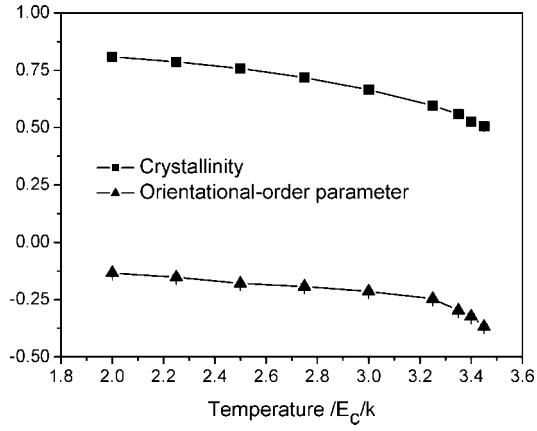

Figure 2. Crystallinities and orientational-order parameters yielded after saturated isothermal crystallization under soft confinement at variable low temperatures.

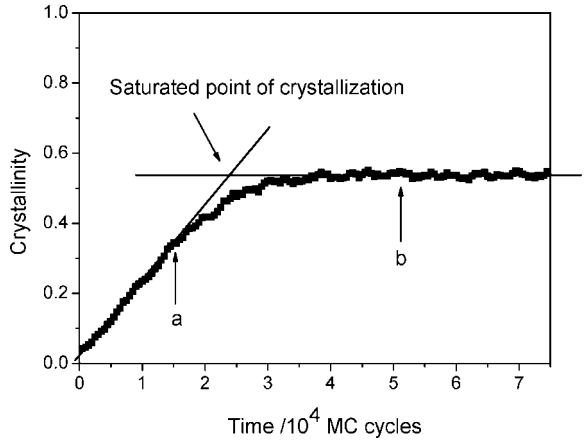

Figure 3. Time evolution of crystallinity for the cylindrical diblock copolymers on isothermal crystallization under soft confinement at $kT/E_c = 3.35$, $E_p/E_c = 1$, $B/E_c = 0.4$, and $E_r/E_c = 0$. The saturated point of crystallization is defined by the interception between the transition curve and the horizontal curve as drawn to guide the eyes. Two vertical arrows indicate the time periods at which the snapshots have been made for Figure 4.

making the interception between the curves extrapolated from the transition region and from the horizontal region.

The morphologies of the sample system in Figure 3 were also traced by visual inspections on the snapshots obtained during isothermal crystallization. The interesting result is that the probability to observe both the breakout and breakdown becomes high in the time period around the saturated point of crystallization. Figure 4a,b demonstrates two snapshots obtained separately before and after the saturated point of crystallization. One can see from Figure 4a that the cylinders are preserved well although some extent of undulation (green circles), and the occasional breakout (the red circle) can be observed due to the effect of overcrowding at interfaces, as discussed in the previous report.[13] In Figure 4b, both breakout and breakdown abundantly occur after crystallization has been saturated. A movie showing this process has been made available as Supporting Information.

The structure factors during the above isothermal crystallization were also traced, as shown in Figure 5. One can see that in the initial state the typically hexagonal packing of cylinders exhibits two small peaks at the wave vectors of the square roots of four and seven, respectively, with reference to the wave vector of the highest peak. One interesting observation is that around the saturated point of crystallization the peak at the square root of seven disappears. This observation suggests

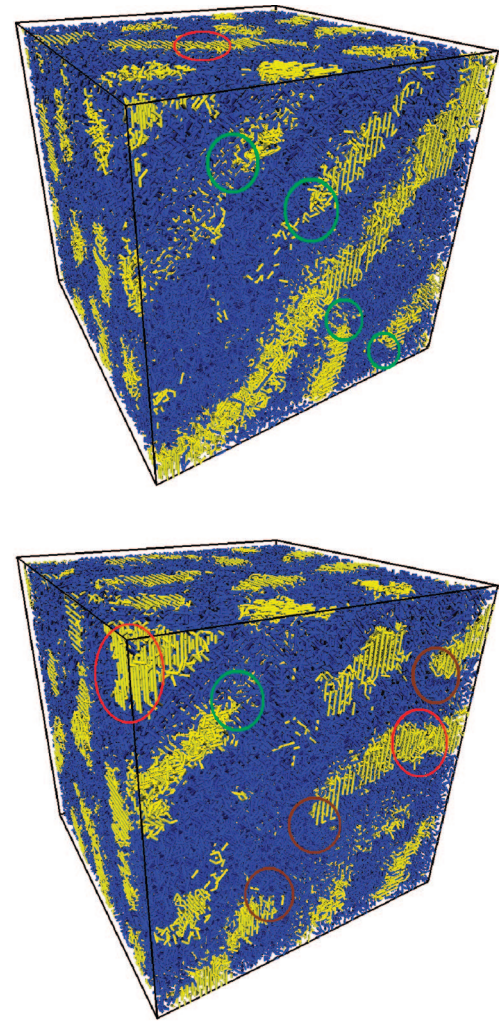

Figure 4. Snapshots of the sample system after isothermal crystallization under soft confinement at $kT/E_c = 3.35$, $E_p/E_c = 1$, $B/E_c = 0.4$, and $E_r/E_c = 0$ for (a) 15 000 and (b) 52 000 MC cycles. All the crystallizable bonds are drawn in yellow tiny cylinders, and all the noncrystallizable bonds in blue tiny cylinders, in the 64^3 box. The green circles indicate the undulation from the upper side to down side of the sectional surface, the red circles indicate the breakout, and the brown circles indicate the breakdown.

that we can make use of the disappearance of this peak as an indication of the abundant breakout and breakdown. Figure 6 demonstrates the definition of the saturated point of the breakout as the interception between two curves extrapolated from the transition region and from the finished horizontal region separately. Here, for the sake of simplicity, we named this saturated point as only the breakout although both the breakout and breakdown may occur simultaneously.

Now, we expanded the above observations to the whole temperature range for isothermal crystallization in both cases without any restriction ($E_r/E_c = 0$) and with a strong restriction ($E_r/E_c = 0.3$) for sliding diffusion of the chains in the crystalline phase. The saturated points of crystallization and breakout are summarized in Figure 7. One can see that a strong restriction for sliding diffusion of chains in the crystalline phase contributes to the stability of crystals and thus makes a shift of the curves to higher temperatures. The saturated points of crystallization cross over those of breakout at a relatively high temperature that splits the temperature region into two. Above the crossing point, the breakout occurs during crystal growth, and below this point, the breakout occurs during the postgrowth isothermal annealing. In the case with a strong sliding restriction, no more

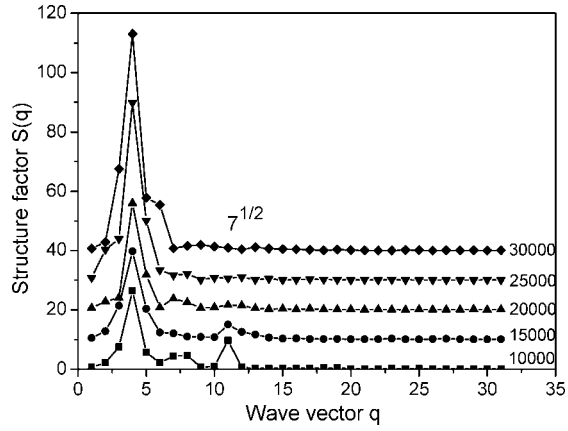

Figure 5. Time-evolution curves (labeled with units of MC cycles) of collective structure factors on isothermal crystallization under soft confinement at $kT/E_c = 3.35$, $E_p/E_c = 1$, $B/E_c = 0.4$, and $E_r/E_c = 0$ for the cylindrical diblock copolymers. The peak at the square root of seven referenced to the wave vector of the highest peak disappears with time evolution. The curves are shifted vertically with parallel offsets for clarity. The segments are drawn to guide the eyes.

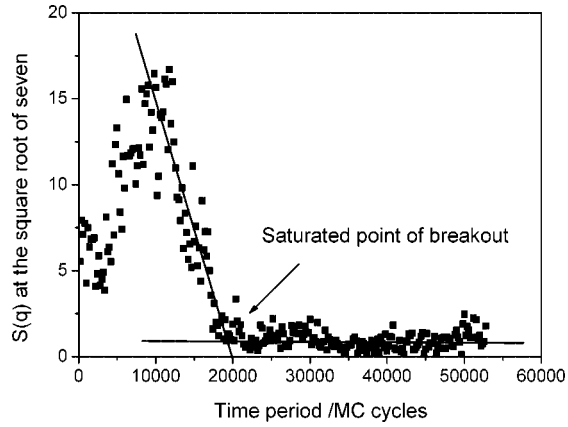

Figure 6. Time evolution of structure factors at the square root of seven referenced to the wave vector of the highest peak of structure factors for the sample system same as in Figure 5. The lines extrapolated from the transition region and from the horizontal region are drawn to guide the eyes.

breakout occurs below the crossing point although crystallization still happens with very small saturated points unmeasured in Figure 7.

In the cases without any restriction of sliding diffusion ($E_r/E_c = 0$), the breakout occurs below the crossing point after crystal growth has been saturated, i.e. in the isothermal annealing process, while in the cases with a strong restriction ($E_r/E_c = 0.3$) there is no more breakout. These different behaviors imply that the breakout at low temperatures is related with the sliding diffusion of polymers in the crystalline phase, which is responsible for the crystal thickening upon isothermal annealing after crystal growth. The similar mechanism has been found in the coalescence of lamellar microdomains of diblock copolymers, where perpendicular preferences of crystal orientation favor the breakout via crystal thickening at high temperatures.[13] We made a snapshot of the present system at the low temperature 2.0 after the breakout has occurred, as shown in Figure 8. In this snapshot, at the upper-left corner of the front face, one can see coalescence of two crystallites with the same crystal orientations via crystal thickening. A few cylinders can be preserved well at low temperatures.

At high temperatures above the crossing point, the breakout occurs before crystallization has been saturated in both cases

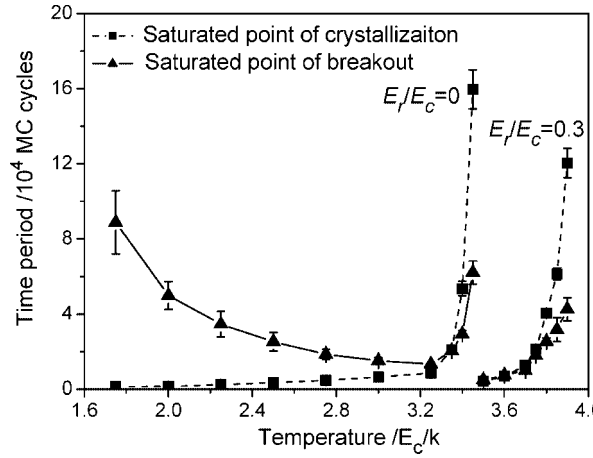

Figure 7. Saturated points of crystallization and breakout as denoted on isothermal crystallization under soft confinement at variable temperatures for the cylindrical diblock copolymers. Each data is averaged over five individual observations (different seeds for random number generation). The segments are drawn to guide the eyes.

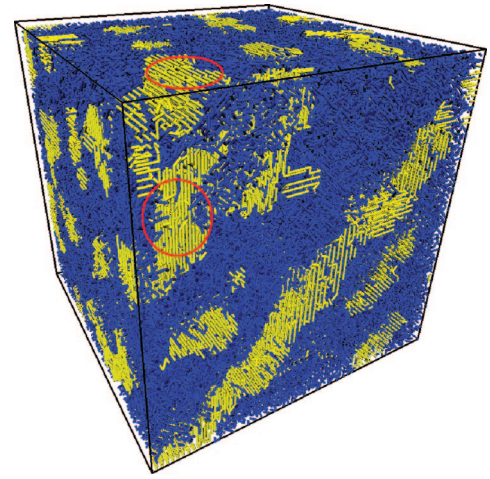

Figure 8. Snapshot of the sample system after isothermal crystallization under soft confinement at $kT/E_c = 2.0$, $E_p/E_c = 1$, $B/E_c = 0.4$, and $E_r/E_c = 0$ for 90 000 MC cycles. All the crystallizable bonds are drawn in yellow tiny cylinders, and all the noncrystallizable bonds in blue tine cylinders, in the 64^3 box. The breakout occurs at the upper-left corner of the front sectional face, as indicated by the red circles.

with and without the postgrowth crystal thickening. This priority of the breakout implies that crystal growth rather than postgrowth isothermal thickening of the lamellar crystallites becomes responsible for the observed breakout. Crystal thickening via sliding diffusion appears no more relevant with the occurrence of the present breakout. Again, we made a snapshot of the sample system at the high temperature 3.75 after the observed breakout has occurred in the case with a strong restriction of crystal thickening, as shown in Figure 9. To our surprise, we mainly observed the breakdown here. At the front sectional surface, one can see a string of small crystallites, and inside each crystallite the orientations of crystalline bonds are quite uniform. This result is consistent with the reported experimental observation at high temperatures.[12] Since the crystal thickening has been blocked in the present case, the observed breakdown can be attributed to the fact that at high temperatures the growing thickness of those tilted or perpendicular-oriented crystals can be so large, even beyond the thickness of cylinders. Meanwhile, at high temperatures, the crystals favor more the perpendicular orientations, as revealed in Figure 2. The combination of these results implies that when the growing thickness of crystals with preferred tilted or perpendicular orientations becomes larger than

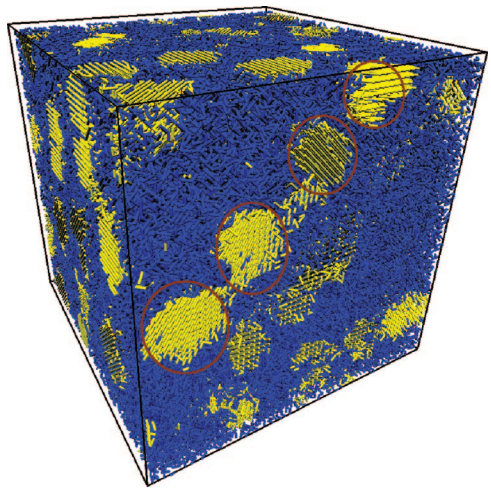

Figure 9. Snapshot of the sample system after isothermal crystallization under soft confinement at $kT/E_c = 3.75$, $E_p/E_c = 1$, $B/E_c = 0.4$, and $E_r/E_c = 0.3$ for 50 000 MC cycles. All the crystallizable bonds are drawn in yellow tiny cylinders, and all the noncrystallizable bonds in blue tine cylinders, in the 64^3 box. The brown circles indicate the breakdown on the cylinder.

the cylinder thickness, the cylinders have to break down the continuity along their long axis and turn into strings of small crystallites in order to maintain the almost constant total volume of the crystallizable phase. Therefore, the lateral crystal growth of a large crystal thickness, together with the tilted and perpendicular crystal orientations, appears as responsible for the occurrence of the breakdown at high temperatures.

IV. Conclusions

By means of dynamic Monte Carlo simulations, we visualized the breakout and breakdown induced by crystallization that was softly confined in the cylindrical microdomains of asymmetric diblock copolymers. In comparison of the cases with and without the postgrowth crystal thickening, we found that the breakout can be assigned to the postgrowth thickening of those crystals with their orientations preferring to stretch out of the cylinders, while the breakdown can be attributed to the lateral growth of these crystals with the growing thickness larger than the thickness of cylinders. Such a microscopic understanding of the breakout and breakdown may shed lights on the morphological control in the crystallization of cylinder-forming diblock copolymers.

Acknowledgment. W.H. thanks the helpful discussions from Günter Reiter at Freiburg University, Germany. The financial support from Chinese Ministry of Education (NCET-04-0448) and National Natural Science Foundation of China (NSFC Grant No. 20474027, 20674036) is appreciated.

Supporting Information Available: Movie made by the snapshots obtained from 15 000 to 50 000 with 1000 MC cycle intervals for the cylinder-forming diblock copolymers during isothermal crystallization under soft confinement at $kT/E_c = 3.35$, $E_p/E_c = 1$, $B/E_c = 0.4$, and $E_r/E_c = 0$; all the crystallizable bonds drawn in yellow tiny cylinders, and all the noncrystallizable bonds in blue tine cylinders, in the 64^3 box. This material is available free of charge via the Internet at http://pubs.acs.org.

References and Notes

(1) Martin, C. R. *Science* **1994**, *266*, 1961.
(2) Martin, C. R. *Chem. Mater.* **1996**, *8*, 1739.
(3) Cepak, V. M.; Martin, C. R. *Chem. Mater.* **1999**, *11*, 1363.
(4) De Rosa, C.; Park, C.; Thomas, E. L.; Lotz, B. *Nature (London)* **2000**, *405*, 433.
(5) Ma, Y.; Hu, W.-B.; Hobbs, J.; Reiter, G. *Soft Matter* **2008**, *4*, 540.
(6) Nojima, S.; Kato, K.; Yamamoto, S.; Ashida, T. *Macromolecules* **1992**, *25*, 2237.
(7) Ryan, A. J.; Hamley, I. W.; Bras, W.; Bates, F. S. *Macromolecules* **1995**, *28*, 3860.
(8) Hillmyer, M. A.; Bates, F. S. *Macromol. Symp.* **1997**, *117*, 121.
(9) Quiram, D. J.; Register, R. A.; Marchand, G. R. *Macromolecules* **1997**, *30*, 4551.
(10) Quiram, D. J.; Register, R. A.; Marchand, G. R.; Ryan, A. J. *Macromolecules* **1997**, *30*, 8338.
(11) Hsu, J.-Y.; Hsieh, I.-F.; Nandan, B.; Chiu, F.-C.; Chen, J.-H.; Jeng, U.-S.; Chen, H.-L. *Macromolecules* **2007**, *40*, 5014.
(12) Vasilev, C.; Reiter, G.; Pispas, S.; Hadjichristidis, N. *Polymer* **2006**, *47*, 330.
(13) Hu, W.-B. *Macromolecules* **2005**, *38*, 3977.
(14) Wang, M.-X.; Hu, W.-B.; Ma, Y.; Ma, Y. Q. *J. Chem. Phys.* **2006**, *124*, 244901.
(15) Zhu, L.; Chen, Y.; Zhang, A.; Calhoun, B. H.; Chun, M.; Quirk, R. P.; Cheng, S. Z. D.; Hsiao, B. S.; Yeh, F.; Hashimoto, T. *Phys. Rev. B* **1999**, *60*, 10022.
(16) Hu, W.-B.; Frenkel, D. *Adv. Polym. Sci.* **2005**, *191*, 1.
(17) Hu, W.-B. *J. Chem. Phys.* **2001**, *115*, 4395.
(18) Hoffmann, A.; Sommer, J.-U.; Blumen, A. *J. Chem. Phys.* **1997**, *107*, 7559.
(19) Zhu, L.; Mimnaugh, B. R.; Ge, Q.; Quirk, R. P.; Cheng, S. Z. D.; Thomas, E. L.; Lotz, B.; Hsiao, B. S.; Yeh, F.; Liu, L. *Polymer* **2001**, *42*, 9121.

MA801097Y